NPL Report MATC (A) 11

# An Experimental Validation of Modelling for Pb-free Solder Joint Reliability

**Miloš Dušek, Jaspal Nottay and Christopher Hunt**

**Hua Lu, Christopher Bailey, University of Greenwich**

**October 2001**

October 2001

# An Experimental Validation of Modelling for Pb-free Solder Joint Reliability

Miloš Dušek, Jaspal Nottay and Christopher Hunt
National Physical Laboratory
Hua Lu, Christopher Bailey, University of Greenwich

ABSTRACT

Assessing/predicting the reliability of solder joints on electronic components has traditionally involved accelerated thermal cycling. However, such testing can be time-consuming and expensive since one cycle can be as long as an hour and it may take thousands of cycles before failure of the joint. Any test procedures, say using computer modelling, to shorten this evaluation period will therefore offer significant benefits to the industry.

This report presents the findings of an initial collaborative study of the use of a particular software-model combination to predict trends in solder joint failures and compare them with those observed experimentally. In the latter, the joints, which were made using two lead-free solders, were stressed using four different thermal cycling regimes, including one typical of that used in automotive products and the other appropriate for military equipment. The results were benchmarked against those obtained using conventional SnPb solder. The findings are encouraging in that the model successfully predicted the failure trends observed in the joints and hence forms a good base for further stages of the work. Differences in the absolute numbers of cycles to failure observed experimentally and predicted theoretically are attributed to the sensitivity of the constitutive equations used and the fact that the model (knowingly) did not take crack propagation into account. The results indicate that the joints associated with a simple 2512-type resistors provide a good test vehicle for this type of study. Moreover, the findings demonstrate that a 3D modelling approach is essential to characterise the changing stress and strain patterns experienced by the joint through each thermal cycle.

ISSN 1361-4061

National Physical Laboratory
Teddington, Middlesex, UK, TW11 0LW



Approved on behalf of Managing Director, NPL, by Dr C Lea,
Head, Materials Centre

**CONTENT**

# 1. INTRODUCTION

A conventional method for assessing reliability of solder joints is to use electrical continuity measurement. Although this method provides a technique in which a large number of joints can be monitored, it is dependent on a complete electrical open circuit occurring before any failure is registered. This can be a severe handicap when over 5000 cycles (~6+ months experiment) may be required to reach failure. To reduce the experimental time in assessing a solder alloy, components are selected which are known to be more prone to solder joint failure, often referred to as "weak links". Typically with these components the coefficient of thermal expansion CTE mismatch is high, and in this study 2512-type ceramic resistors and large BGAs were used.

These "weak link" components are the most likely to suffer solder joint failure in commercial products. Thermal cycling drives the development of cracks and structural changes that will weaken a solder joint. Since electronics assemblies are manufactured from various materials with different CTEs, shear strains are placed on the various components in the assembly as it is taken through a thermal cycle. This is shown schematically in Figure 1. Temperature cycling during service induces stresses due to the CTE differences between the mounted component and base substrate, and it is a function of the materials used in electronic assemblies that this strain is relieved in the solder joint. The strain is relieved by microstructural changes and the development of cracks, which accumulate as a consequence of continual cycling.

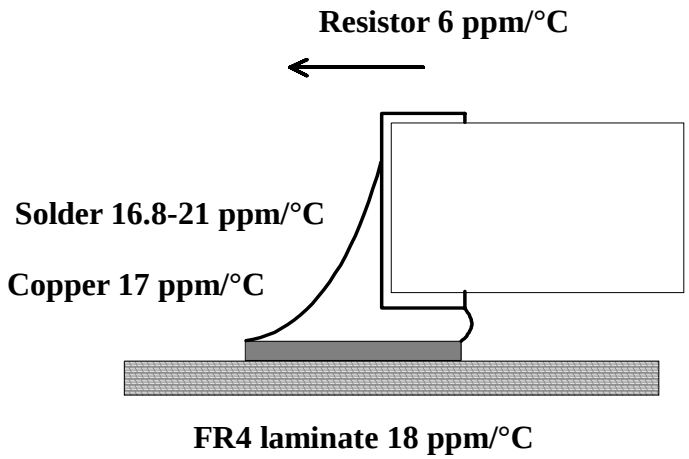


**Figure 1: CTE (X-axis) of materials used in SM assemblies**

SnPb solders have been widely used in the electronics industry for a long time. However, their toxicity gave rise to proposals for anti-lead legislation in the USA more than ten years ago. These proposals, although rebutted at that time, have created a momentum for lead-free electronics, which shifted to Europe, and has led to the incorporation of lead-elimination measures in the EU's WEEE Directive. This Directive aims firstly at the prevention of waste from electrical and electronic equipment, secondly at the re-use, recycling and other forms of recovery of such wastes, and thirdly at minimising the risks and impacts to the environment associated with the treatment and disposal of end-of-life electrical and electronic equipment. The identification and introduction of suitable lead-free solders is now a major area of research in the electronics industry.

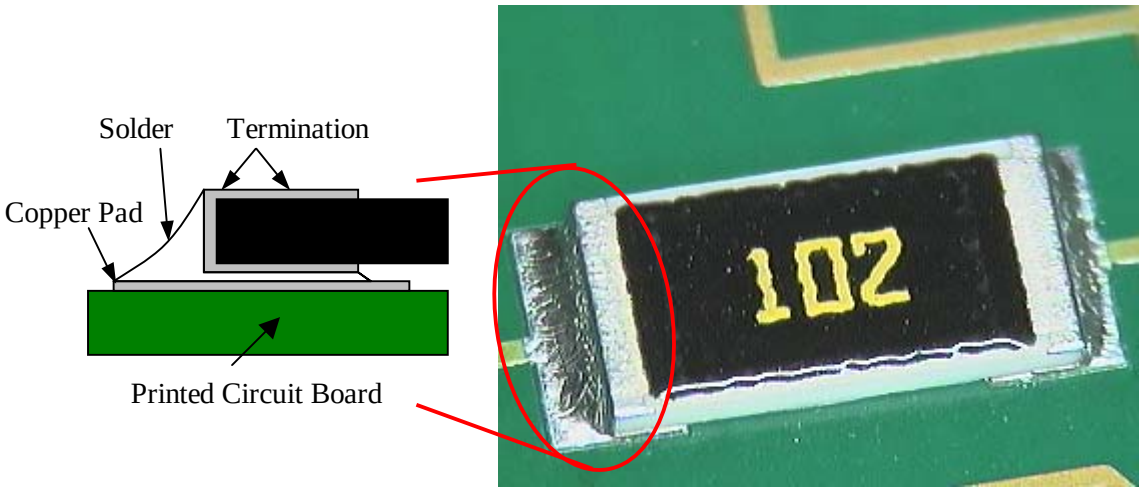


**Figure 2 Solder joint of 2512-resistor**

## 2. OBJECTIVES AND TEST VEHICLE

In developing a successful model for predicting the reliability of solder joints it is important to use materials data obtained from realistic solder joints i.e. from joints having dimensions and geometries reflecting those in actual surface mount products. As part of a previous programme NPL has developed an instrument for obtaining such data – the electro-thermal mechanical tester (ETMT – see reference 13) – and it is to be used for data collection in later stages of this work. As a preliminary exercise, however, other data collected as part of a larger programme, have been used to test this particular software-model combination.

The prime objective of this work was to investigate whether the particular combination of modelling software (PHYSICA) and the model for fatigue and creep behaviour developed at Greenwich University could successfully predict the failure trends observed experimentally using a proven test vehicle. The latter employed surface mount 2512-type resistors (used extensively on PCBs in the electronic industry) with joints soldered using two lead-free alloys and stressed using four different thermal cycling profiles. Conventional SnPb soldered joints were used to benchmark both the data collected and the application of the model.

The details of the resistor-PCB combination are shown in Figure 2. The resistor is connected to the PCB at each end, where solder (either tin-lead eutectic or lead-free) has flowed up the side of the resistor, and under the termination and between the pads on the PCB. The fillet shape, its curvature, and resultant stand-off height of the resistor above the PCB are dependent on solder volume used, the termination solderability and surface tension of the solder. Different fillet shapes for the two materials may affect the reliability and hence impact on the successful introduction of a lead-free solder for this component.

With only two connections to the PCB, resistors are relatively simple components to model, compared to multi interconnection components such as BGA (ball grid array) and FC (flip-chip) packages. Nonetheless, the reliability of these two resistor solder joints is by no means less of a challenge to model in terms of predicting thermal-mechanical fatigue of the solder joints. Important parameters that influence the failure mode are solder volume, fillet shape, stand-off height, and component material properties (i.e. Young's Modulus, coefficient of thermal expansion, etc).

Because the resistors and the PCB are made from materials with different coefficient of thermal expansion (CTE), cyclic temperature changes will produce cyclic stresses and strains in the solder joints and these cyclic loads may lead to crack initiation and propagation. It should be noted that other failure mechanisms could occur, such as resistor cracking or delaminating at material interfaces. In this modelling analysis only solder fatigue damaging mechanisms are considered.

In Figure 3 a micrograph of a typical cross-section of a 2512-resistor solder joint is shown. This component failed during a thermal cycling test. Experimental observation of SnPb solder interconnections indicates that cracks usually initiate in the solder between the resistor body and the PCB. This crack then propagates through the solder fillet eventually to emerge on the surface of the solder fillet to cause total detachment between the resistor and PCB. Solder joint lifetimes are typically expressed as the number of thermal cycles that a solder joint experiences when 62.3% of the tested joints fail, called $N_f$.

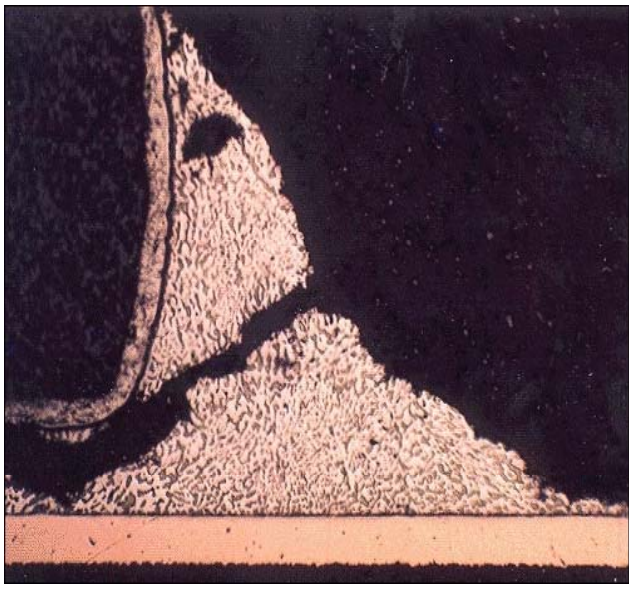

**Figure 3: Micrograph of the cross section of a cracked 2512-resistor**

Computational modelling is now acknowledged as an equal and long-term indispensable partner, along with theory and experiment, in the advance of scientific knowledge and engineering practice. Numerical simulation enables the study of complex systems and natural phenomena that would be too expensive, or even impossible, to study by direct experimentation. Stress predictions, using finite element calculations, have been undertaken by a number of groups to predict thermal stress and fatigue in solder joints for a number of components [1]. These types of simulations are very dependent on the input they require. A part of this data set is the physical properties of the materials being analysed - both thermal and mechanical. In this study the same geometries have been modelled as tested in the experimental work. These dimensional data and other materials data were fed into the models for SnPb and SnAgCu solders

## 3. MODELLING METHODOLOGY

The modelling software PHYSICA [8] solves partial differential equations, representing the governing physics in a process, by dividing the 3D domain into a collection of related discrete elements and approximating the continuous variables by finite number of discrete variables [9]. These equations are then partitioned using appropriate methods to obtain a system of equations, which with appropriate boundary conditions can be solved to provide thermal and stress data across a component.

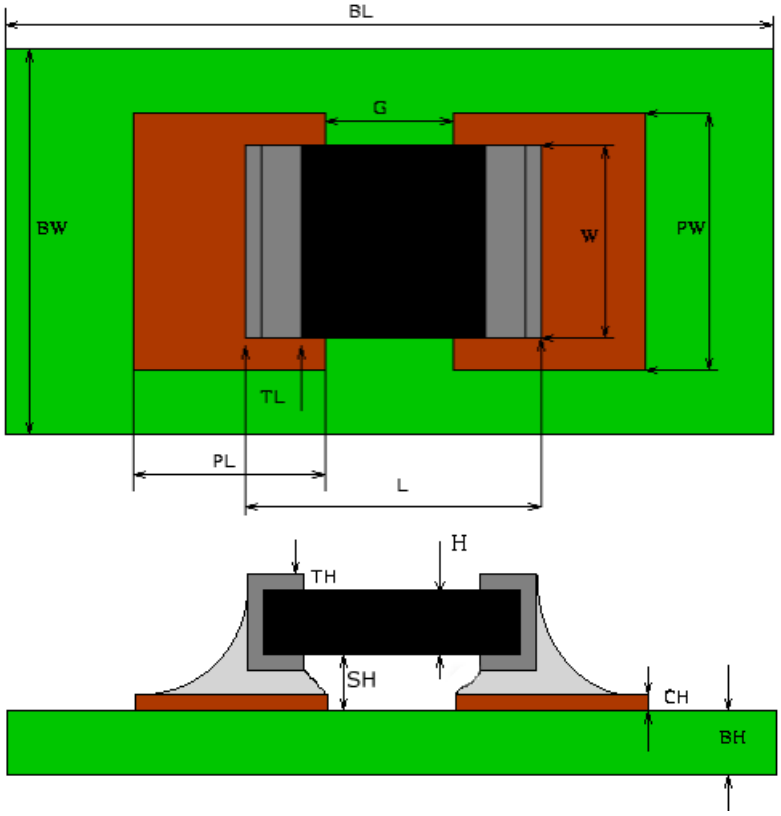


**Figure 4 Definition of resistor model dimensions**

**Table 1: Resistor model dimensions**

| | |
|---|---|
| L | 6.21mm |
| W | 3.11mm (width) |
| TL | 0.56mm (termination) |
| H | 0.55mm (thickness) |
| SH | 80 micons, (standoff height) |
| G | 4.45 mm (gap) |
| PL | 1.68 mm (pad length) |
| PW | 3.15 mm (pad width) |
| BL | 16 mm |
| BW | 8 mm |
| TH | 20+5 microns |
| CH | 35 microns |
| BH | 1.6 mm |

Based on the resistor's dimensions, shown in Figure 4 and Table 1, a three-dimensional computer model was built. The outline and a cross section of this can be seen in Figure 5, where the different materials are clearly illustrated. This model uses experimental data such as solder fillet shape and standoff height, which were measured. Because of the domain symmetry, only one quarter of the resistor is represented in the model. The rest of the resistor can be accounted for by symmetry boundary conditions.

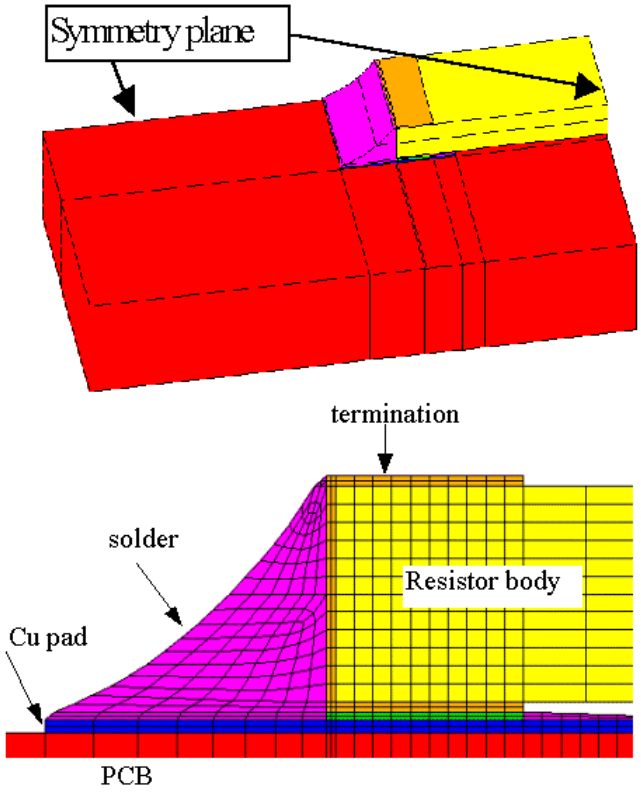


**Figure 5: Top: The outline of a ¼ model of the 2512-resistor.**
**Bottom: A cross section of the computer model of the 2512-resistor**

The solder is assumed to behave as an isotropic elasto-viscoplastic material and the board is assumed to be orthotropic and elastic. Other materials in the domain are assumed to be isotropic and elastic. The model includes the most relevant parameters for the mechanical behaviour of the assembly. The mechanical properties used in this analysis are listed in Table 2. The model calculates the accumulated creep strain energy in the solder during a thermal cycle and the number of cycles ($N_f$) to 62.3% population failure rate is estimated for SnPb solder.

**Table 2: The mechanical-elastic properties of the materials of the leadless SM resistor**

| Material | E elastic modulus (GPa) | Poisson's ratio | CTE (ppm / °C) |
|---|---|---|---|
| 60Sn40Pb | 10 | 0.4 | 16.8-21 |
| 95.8Sn3.5Ag0.7Cu | 50.3 | 0.4 | 28 |
| Alumina (resistor) | 282.7 | 0.22 | 6 |
| Cu (pad) | 121 | 0.35 | 17 |
| FR4 (PCB) | 22 | 0.28 | 18(xy), 70(z) |
| Ag (termination) | 83 | 0.37 | 18.9 |

To model the creep behaviour of solder, the following **constitutive relationship** (1) is used [11, 12]:

$$\frac{d\varepsilon_{cr}}{dt} = \gamma \times \sinh^{n}(\alpha\sigma_{e}) \exp(\frac{-Q}{RT}) \quad (1)$$

where:
$d\varepsilon_{cr}/dt$ is the scalar creep strain rate
T is absolute temperature in K
$R=8.3\ J.K^{-1}.mol^{-1}$ is the gas constant
$\sigma_e$ is the von Mises effective stress in Pa
$\gamma$, $\alpha$, n and Q represent material dependent parameters

For the near eutectic SnPb solder, $\gamma=9.62x10^{4}\ s^{-1}$, $\alpha=0.087\ MPa^{-1}$, n=3.3 and $Q = 66884.471\ J.mol^{-1}$ according to Darveaux [11].

The equation 1 is part of the tensor form of equation 2, which is used in the modelling creep strain rate:

$$\frac{d\varepsilon_{ij}^{cr}}{dt} = \frac{3}{2}\frac{d\varepsilon_{cr}}{dt}\frac{s_{ij}}{\sigma_{e}} \quad (2)$$

where:
$\varepsilon_{ij}^{cr}$ is the creep strain tensor
$s_{ij}$ is the deviatoric stress tensor (stress without hydrostatic part [11])
$\sigma_e$ is the Von Mises effective stress given in equation 3

$$\sigma_{e} = \sqrt{(3/2)s_{ij}s_{ij}} \quad (3)$$

The correlation between plastic energy dissipation density during a thermal cycle and the number of cycles to crack initiation in SnPb solder [11], $N_0$, this is given by:

$$N_0 = 5.42 \times 10^7 / \Delta W \tag{4}$$

The crack propagation rate (5) can be expressed as:

$$\frac{dA}{dN} = 1.745 \times 10^{17} \Delta W^{1.19} \tag{5}$$

where:
A is the cracked area
N is the number of thermal cycles
ΔW is the creep energy dissipation per unit volume accumulated over a thermal cycle

The ΔW can be calculated as a function of the cracked area (length), so the number of cycles for crack propagation through the solder area can be obtained from equation 5. The total lifetime ($N_f$) for SnPb solder joint is estimated from joined equations 4 and 5 as shown in 6.

$$N_f = N_0 + \frac{A}{1.745 \times 10^{17} \Delta W^{1.19}} \tag{6}$$

where:
A is the total area in which the crack can propagate
$N_f$ is characteristic life-time (number of cycles to 62.3% failure rate)
$N_0$ is number of cycles for crack initiation
ΔW is the creep energy dissipation per unit volume accumulated over one thermal cycle

For expressing the damaging effect of accelerated aging (thermocycling) **the volume weighted average (V.WA.)** value of ΔW (Equation 7) is used [6].

$$\Delta W = \frac{\sum_e \Delta W_e V_e}{V_{tot}} \tag{7}$$

where:
$V_{tot}$ is the total volume
$V_e$ is the volume of an element
$\Delta W_e$ is creep energy density within an element
ΔW is the creep energy dissipation per unit volume accumulated over a thermal cycle

This is important for the calculation of $\Delta W_e$ as strain and stress distributions may have peaks or singularities at corners or material interfaces – especially in the solder. The mesh dependency and stress singularity are well known throughout the modelling community and the volume weighted approach provides results that avoid this effect.

The advantage of V.W.A. as compared with **maximum value of the energy density** in the solder is demonstrated in Figure 6, which shows energy density changes in a simplified block of solder material under cyclic thermal loading. Clearly as the mesh density increases, the peak stress at the top right hand corner increases in magnitude. This is shown in the accompanying graph where the energy density significantly increases with mesh density (1, 2, 3). For the V.W.A. approach there is only a small increase in normalized energy as the mesh density

increases from (1)–(2). A finer mesh (3) produces a very small change in volume weighted average energy density as compared with maximal energy density.

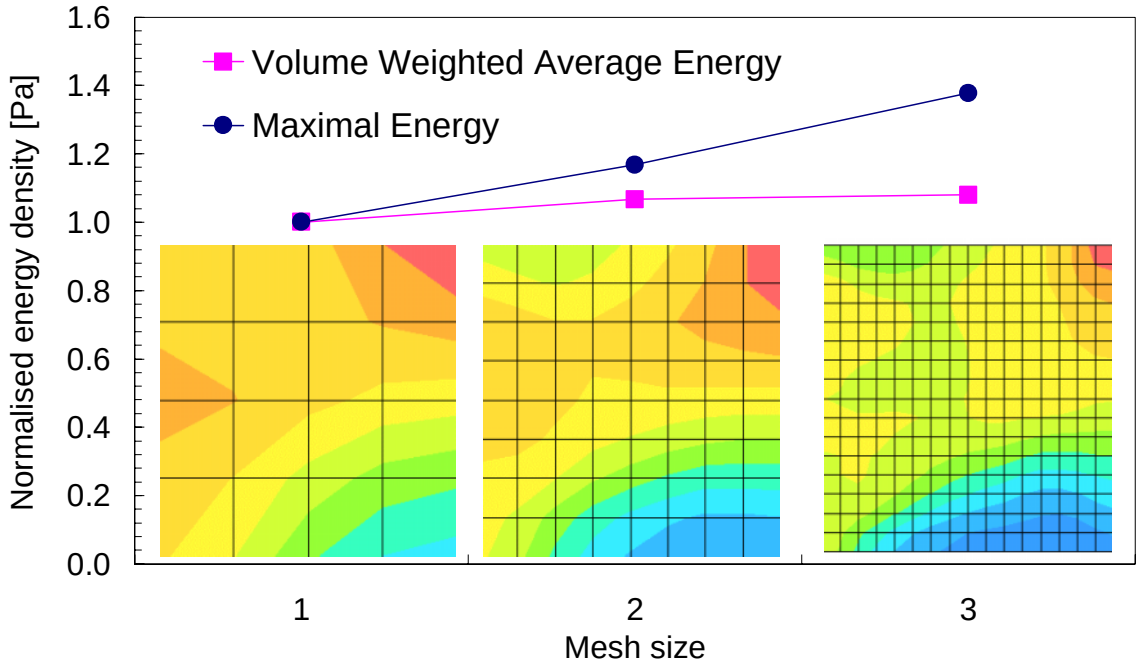


**Figure 6: Energy density of a simplified solder block under shear load**

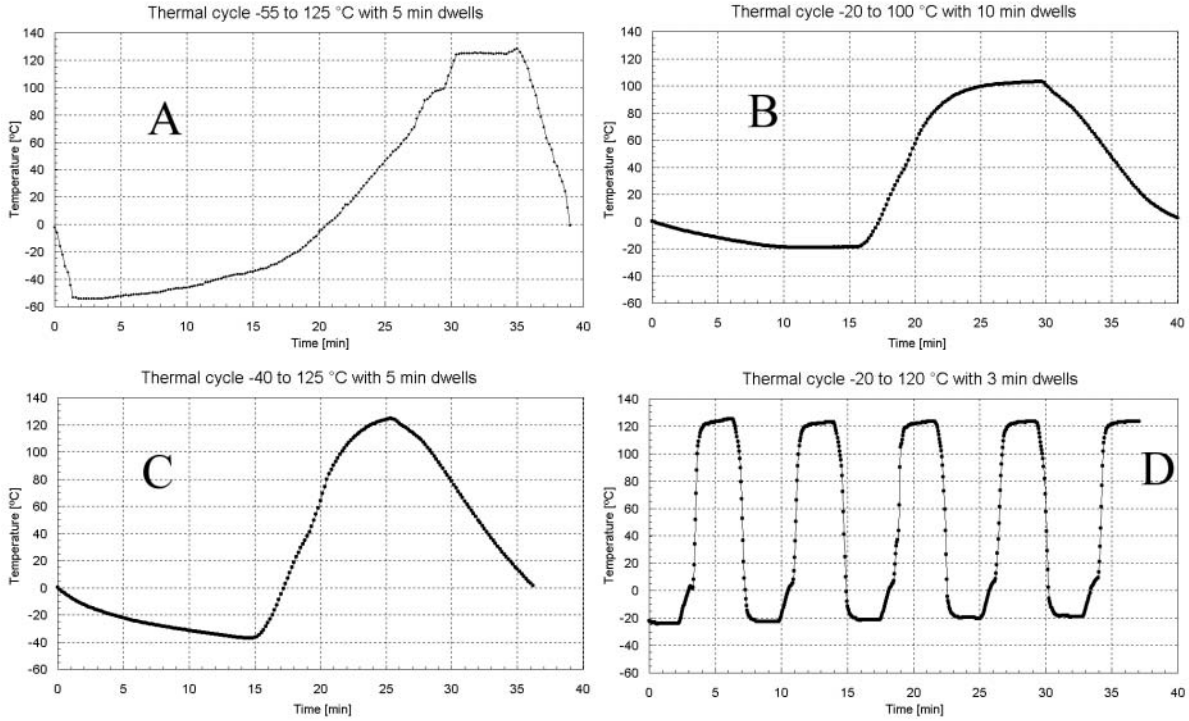


**Figure 7 The temperature profiles of the thermal cycles**

## 3.1 Outcomes of the work

Four different temperature profiles were used as input data for the modelling, and these are shown in Figure 7. The key parameters of these profiles are listed in Table 3.

**Table 3: The parameters of the thermal cycles**

| Temperature profile | Min T [°C] | Max T [°C] | Period [min] |
|---|---|---|---|
| A | -55 | 125 | 40 |
| B | -20 | 100 | 40 |
| C | -40 | 120 | 40 |
| D | -20 | 120 | 7 |

In Figure 8 the stress distribution is shown across the resistor when an assembly is cooled to the low dwell region on the thermal cycle curve (A). As expected, due to the thermal mis-match in the material property data, a high stress region has occurred around the termination and pad. The highest stress is in the Cu pad and the metal termination region. The creep energy dissipation density distribution in the solder joint can be seen in Figure 9. The need for a three-dimensional simulation is highlighted by the creep energy distribution in the volume of the solder joint with a varying damage profile through the width of the solder. Such a variation across the width of the resistor would not be evident from a 2D modelling approach. The region displaying high damage (creep strain energy) is at the edge of the device - situated between the termination and pad at the corner away from the symmetry plane. This predicted location of high damage indicates the most likely spot for crack initiation. The prediction is consistent with experimental observations (microphotographs of cross-section Figure 3), and also appears to suggest that this is the location for crack initiation. After initiation, the crack will first propagate through the whole area between the pad and resistor, and then into the fillet mass - eventually causing total failure of the solder joint.

The concept of two-stage crack propagation is used to calculate total life-time in two steps. In the first step, the model has all the solder material in place and the average value of $\Delta W$ is calculated for the solder volume between the pad on the PCB and the termination on the resistor, V1 in Figure 10. In the second step a new model is constructed with the solder (V1) between the PCB and resistor removed. The creep strain energy, $\Delta W$, is then calculated for the solder volume (V2), which represents the region in which crack propagation will occur at this stage. The total number of cycles for the crack to travel through the two regions (V1 and V2) is then calculated. The total life-time is simply the sum of life-times from these individual regions.

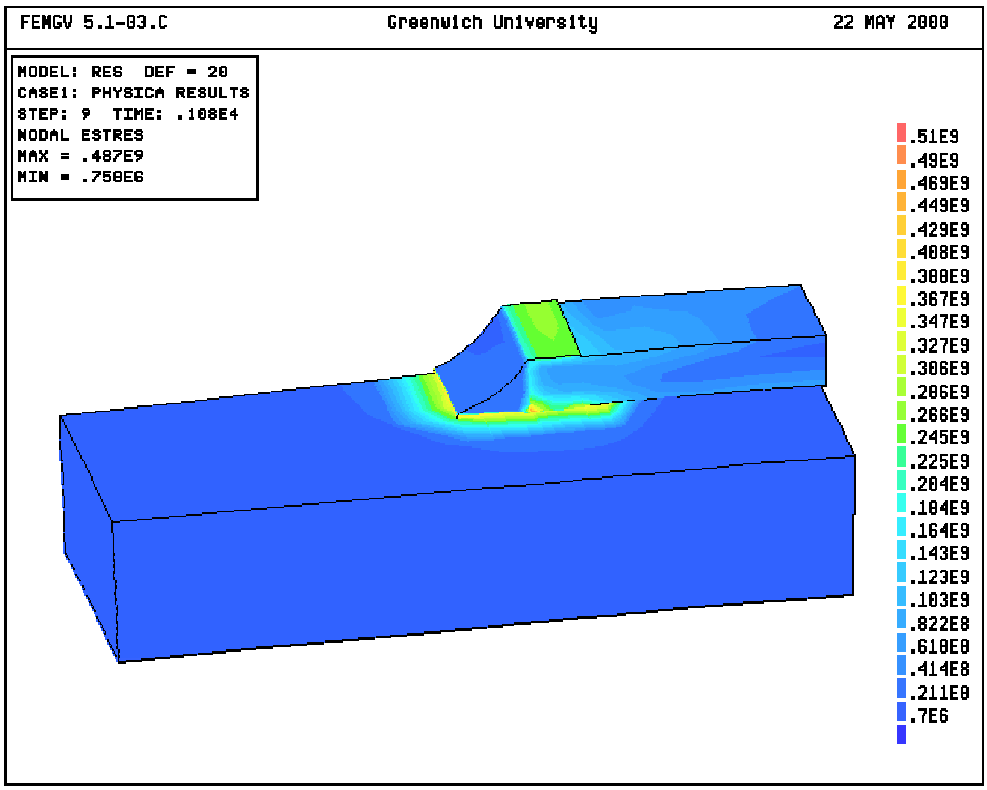


**Figure 8: The stress distribution of the resistor under thermal load. The unit of stress is Pa**

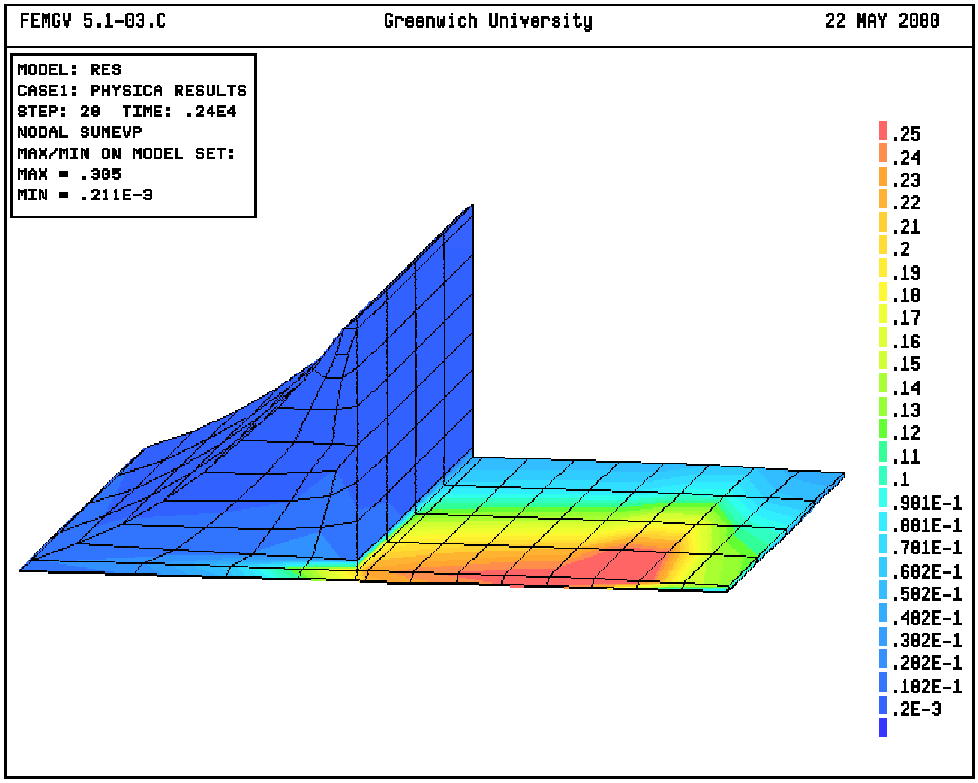


**Figure 9: The creep energy dissipation density distribution at the end of the fifth cycle for temperature profile A. The unit of stress is Pa**

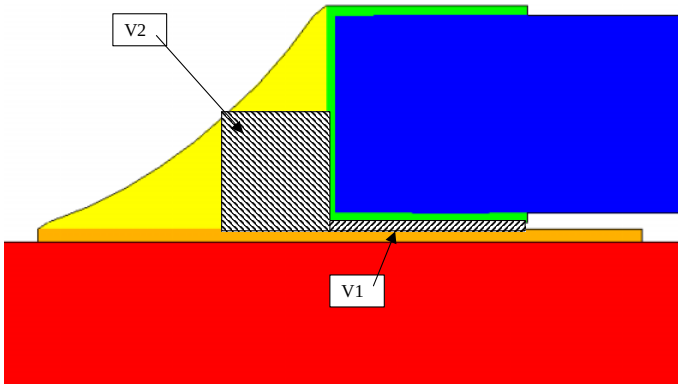


**Figure 10: Cross-section of computer model with volumes V1 and V2**

The data presented in Figure 11 show that value of ΔW does not change much with the number of temperature cycles. The difference between energies at the end of the first and the second cycle is only 1.25% and that between the second and the third is 0.025%. This behaviour suggests that solder stress relaxes very rapidly compared to the time scale of the thermal cycle. The value of ΔW after the fifth cycle was used to calculate characteristic life-time ($N_f$).

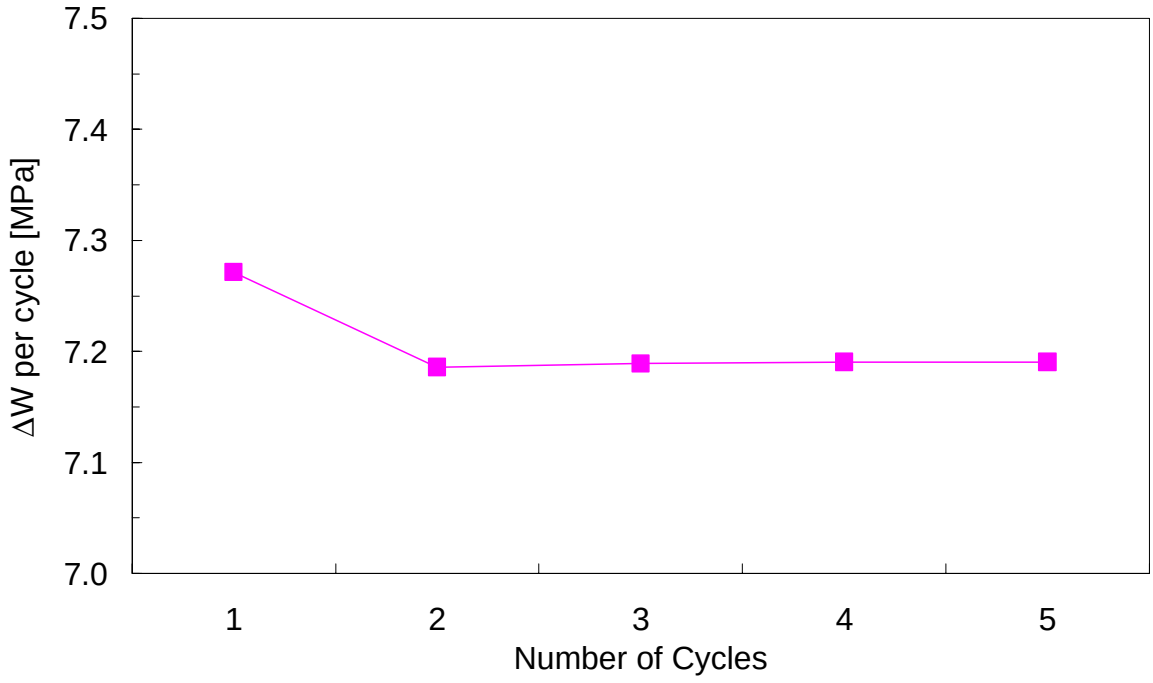


**Figure 11: ΔW as a function of number of thermal cycles.**

The development of the accumulated creep energy densities in region V1 over the first thermal cycle are shown in Figure 12, Figure 13 and Figure 14 for each of the four thermal cycles and three solder alloys. The last reading of each of the data series is defined as the ΔW of this cycle.

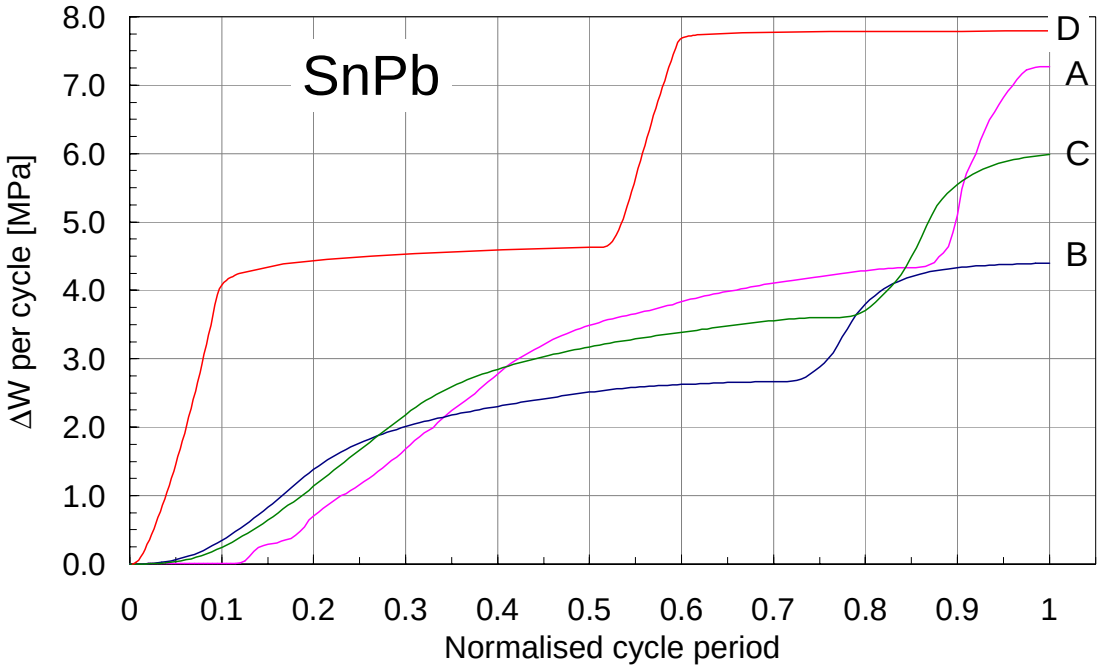


**Figure 12: ΔW between the pad and resistor body as a function of normalized cycle time for SnPb solder alloy and four different thermal cycles**

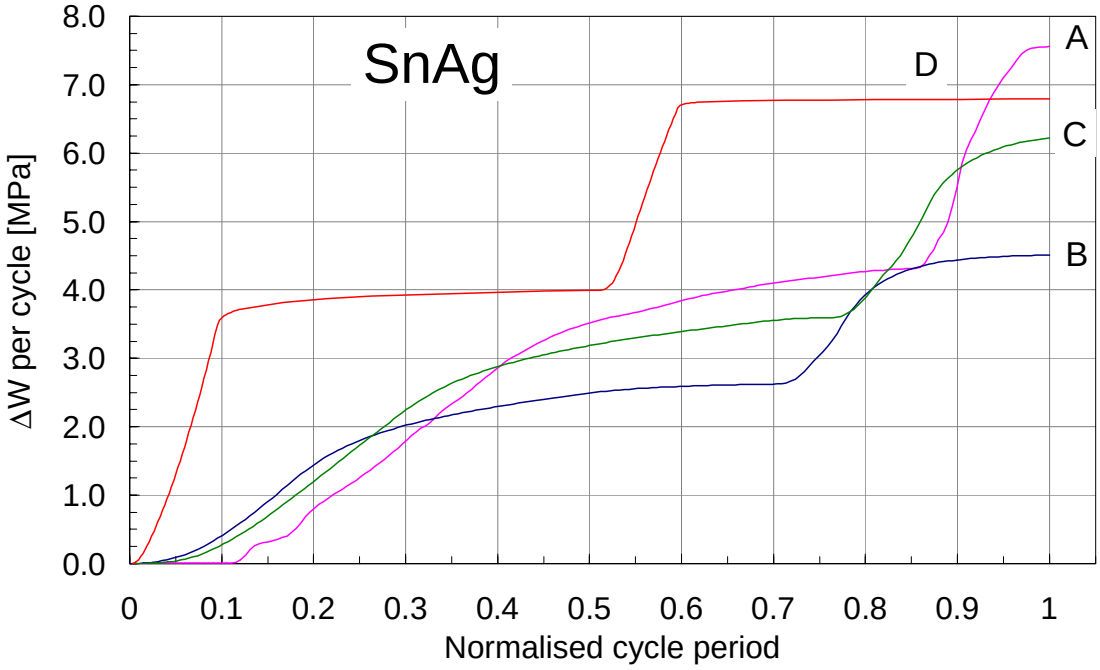


**Figure 13: ΔW between the pad and resistor body as a function of normalized cycle time for SnAg solder alloy and four different thermal cycles**

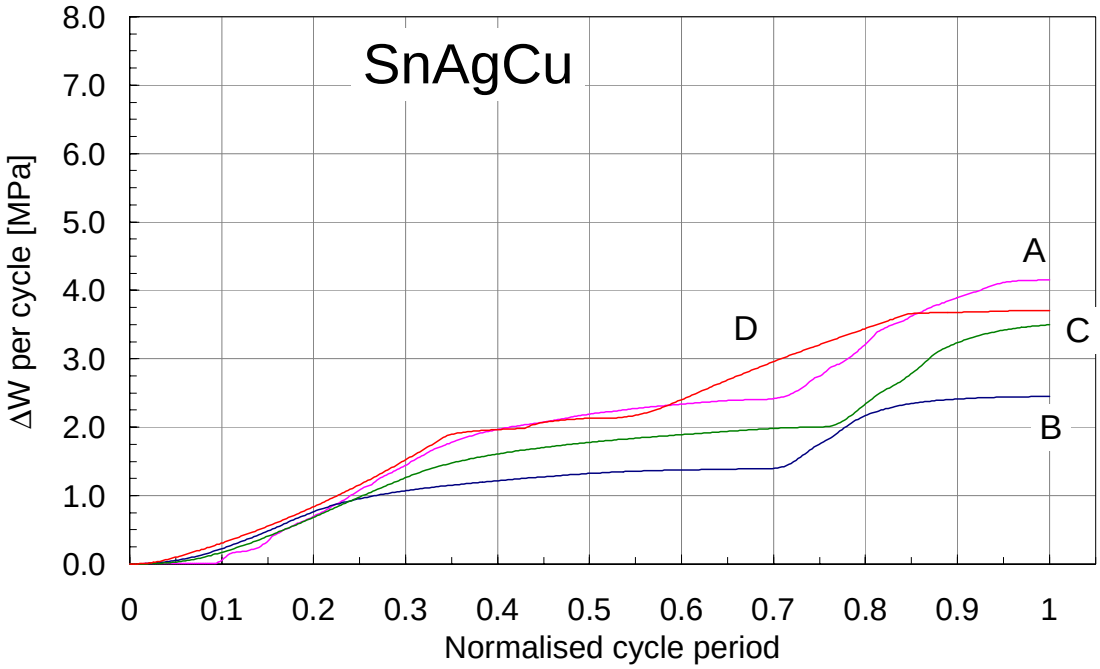


**Figure 14: ΔW between the pad and resistor body as a function of normalized cycle time for SnAgCu solder alloy and four different thermal cycles**

In Table 4 there is the creep energy density ΔW is listed for three types of solder and four different temperature cycles.

**Table 4:**

**The Creep energy density ΔW/cycle of the resistor for four temperature profiles**

| Solder | Volume | Temperature profile | | | |
|---|---|---|---|---|---|
| | | A | B | C | D |
| SnPb | V1 | 7.19 | 4.27 | 5.89 | 7.60 |
| | V2 | 0.55 | 0.34 | 0.46 | 0.54 |
| SnAg | V1 | 7.55 | 4.51 | 6.22 | 6.79 |
| | V2 | 0.60 | 0.36 | 0.50 | 0.56 |
| SnAgCu | V1 | 4.15 | 2.45 | 3.50 | 3.71 |
| | V2 | 0.47 | 0.29 | 0.40 | 0.43 |

The predicted life-times for SnPb solder are summarised in Table 5. In all cases the first stage of crack propagation (**V1**) accounts only for about **4-5%** of the **total life-time**. The relatively short time for the crack to cross the solder between the resistor and PCB is the result of higher stress and strain in this part of the solder material. **The role of the stand-off height here is important as it greatly affects the strain in this region. But since cracks spend much**

**longer in crossing the fillet, the solder joint reliability is much more dependent on the volume and shape of the fillet than on the solder material.**

**Table 5:**

**Mean number of cycles to failure for SnPb solder and four different temperature cycles**

| Profiles | A | B | C | D |
|---|---|---|---|---|
| Nf1 | 220 | 478 | 398 | 201 |
| Nf2 | 5182 | 9381 | 6508 | 5324 |
| Nf(total) | 5402 | 9859 | 6906 | 5525 |
| Days to Failure | 150 | 274 | 173 | 26.9 |

## 4. COMPARISON OF MODELLING RESULTS WITH EXPERIMENTAL DATA

The most common profiles used for reliability evaluation are those based around the military (profile A) and automotive (profile B) applications. Hence for temperature profiles A and B, thermal cycling experiments have been carried to determine the mean life-time of the resistor solder joints. By monitoring the electrical continuity of the 2512-resistors in the oven and from the failure analysis, a Weibull distribution was fitted (Figure 15) to the failure rate. $N_f$, the characteristic numbers of cycles for 62.3 % failure rate, was then estimated. It was found that the mean numbers of cycles to failure are 2998 and 7837 cycles respectively (for A and B profile) see Table 6.

The modelled life-times differ from experimental results as shown in Table 7. The main reason for this discrepancy is perhaps the apparent underestimate of the creep energy dissipation in the solder. As mentioned before, the energy dissipation averaged over V1 and V2, is inevitably smaller than that around the crack tip in reality. To address this problem there should be either new simulation carried out with a crack explicitly inserted, and then energy density calculated along the crack path as the crack propagates, or modify the correlations between crack rate and the dissipation energy.

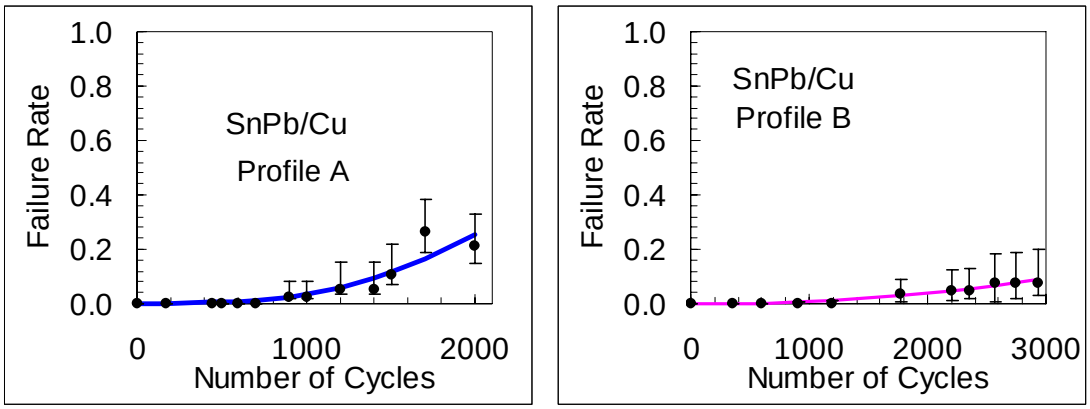

**Figure 15: Weibull distribution fit for 2512-resistors cycled with A and B temperature cycle**

**Table 6: 2512-resistor reliability from experimental testing**

| 2512- Resitor | | |
|---|---|---|
| Temp. profile | Solder/Finish | $N_f$ (62.3%) |
| A | SnPb/Cu | 2998 |
| | SnAgCu/Cu | 1873 |
| B | SnPb/Cu | 7837 |

**Table 7: Comparison of modelling and experimental results for SnPb**

| Temp. profile | A (-55 to 125°C) | | | B (-20 to 120°C) | | |
|---|---|---|---|---|---|---|
| $N_f$ (Experiment) | 2998 | | | 7837 | | |
| FEA modelling | $N_{f1}$ | $N_{f2}$ | $N_{f\ total}$ | $N_{f1}$ | $N_{f2}$ | $N_{f\ total}$ |
| | 220 | 5182 | 5402 | 478 | 9381 | 9859 |
| Ratio Exp./FEA | 13.63 | 0.58 | 0.55 | 16.40 | 0.84 | 0.79 |

## 5. CONCLUSIONS

The salient conclusions of this initial study are:

- The combination of PHYSICA software and Greenwich model was successful in predicting the observed trends in creep behaviour (in terms of the number of cycles to failure) for the two thermal cycling profiles explored.

- This success is encouraging and forms a good foundation for further studies using materials data from realistic solder joints using the ETMT approach. This stage should involve ageing using different thermal cycling profiles, with the objective of understanding how the acceleration profiles alter the rate of failure.

- The differences in the experimentally observed and predicted number of cycles to failure are attributed to the sensitivity of the constitutive relationship used, and the fact that the model does not take crack propagation into account. However, the computing costs associated with including crack propagation in the model are enormous, and hence not appropriate from this study.

- The simple geometries of soldered joints on 2512-type surface mount resistors provide a good test vehicle to progress further work on reliability prediction.

- The modelling results have indicated that, keeping the cycling temperature range constant, the faster the thermal cycling, the fewer the number of cycles to failure. However, this does require experimental validation.

- The modelling results also confirm the findings of earlier work that a 3D modelling approach is essential to characterise fully the changing stress and strain profiles in the solder joints throughout a thermal cycle.

## 6. ACKNOWLEDGEMENTS

The work was carried out as part of a project in the Measurements for the Processability of Materials (MPM7.3) Programme of the UK Department of Trade and Industry.

## 7. REFERENCES

[1] Lau, J. H. "Surface Mount Solder Joints Under Thermal, Mechanical, and Vibration Conditions". *The Mechanics of Solder Alloy Interconnects*, Van Nostrand , New York, NY, 1995, pp361-415

[2] Vincent J.: Improved Design Life and Environmentally Aware Manufacturing of Electronics Assemblies by Lead-Free Soldering: "IDEALS". Synthesis report BE95-1994

[3] Dušek M., Hunt C.: The Impact of Solderability on Reliability and Yield of Surface Mount Assembly, NPL Report CMMT(A)214. Teddington, September 1999

[4] Dušek M., Hunt C.: Optimum Pad Design and Solder Joint Shape for Reliability. NPL Report CMMT(A)215, Teddington, August 1999

[5] Mills K.: Metals Handbook Ninth Edition Volume 9, Metallography and Microstructure. American Society for Metals, 1985, ISBN 0-87170-007-7

[6] Dušek M., Nottay J., Hunt C.: The Use of Shear Testing and Thermal Cycling for Assessment of Solder Joint Reliability. NPL Report CMMT(A)268, Teddington, June 2000

[7] Lau, J. H. "Surface Mount Solder Joints Under Thermal, Mechanical, and Vibration Conditions". The Mechanics of Solder Alloy Interconnects, Van Nostrand , New York, NY, 1995, pp361-415

[8] PHYSICA, V2.10. http://physica.gre.ac.uk

[9] Taylor, G. A.: " A Vertex Based Discretization Scheme Applied to Material Non-Linearity within a Multi-Physics Finite Volume Framework", Ph.D thesis. University of Greenwich, 1997

[10] Frear, D., Morgan, H., Burchett, S. and Lau, J. (editors): The Mechanics of Solder Alloy interconnects. Chapman and Hall, New York, 1994, pp323-324.

[11] Darveaux, R.: "Solder Joint Fatigue Life Model". Design and Reliability of Solders and Solder Interconnections, 1997, pp213-218.

[12] Darveaux, R., Banerji, K.: Ball Grid Array Technology. 1995,McGraw-Hill,pp379-442

[13] Mummery, P. Foroodian, M. Roebuck, B. Thermomechanical Fatigue of Solders. NPL Report CMMT (D) 202, March 1999, Teddington.